Hysteresis Dynamic Behavior of Pneumatic Artificial Muscle

Manuscript received March 29, 2024; revised April 4, 2024

Vo Ngoc Yen Phuong*
Faculty of Mechanical Technology
Industrial University of Ho Chi Minh City
Ho Chi Minh City, Viet Nam
vongocyenphuong@iuh.edu.vn

Trinh Van Chon
Faculty of Mechanical Engineering
Ho Chi Minh City University of Technology
Ho Chi Minh City, Viet Nam
tvchon.sdh221@hcmut.edu.vn

***Abstract*—The purpose of this work paper is to analyze the effects of friction on the hysteresis dynamic behavior of pneumatic artificial muscle (PAM). Due to the structure of the PAM, the dynamic response is not only affected by the compressed air but also the friction phenomenon. Indeed, the pipe of the PAM called the bellow is made from rubber simultaneously reinforced by metal fibers that are wrapped around the bellow. Hence, the effect of the friction between fibers, between fiber and rubber will be considered in the nonlinear dynamic of the PAM. From dynamic analysis, the complex stiffness model will be attained and analyzed. Comparison between the analysis model and experimental results is realized subjected to harmonic displacement excitation. The results proved the effectiveness of the analysis model. The studied model is a suitable tool in the field of systems vibration analysis using PAM as an elastic element, actuator.**

Keywords*—*Friction, Hysteresis Dynamic, Pneumatic Artificial Muscle

I. INTRODUCTION

As known, PAMs have many significant potential applications in engineering thanks to their advantages such as energy efficiencies, force output, and stroke length improvement. Especially the actuator can be allowed to be a structural component. However, there are few studies about it as well as have not focused on increasing the dynamic performance and aim to apply controlling it to enhance the mentioned benefits. For example, in [1] Michael F. et al. implemented an internal pulley mechanism to increase further stroke length of PAM and to reduce the cost of maximum force output. In another study, [2], Michael F. Cullinan et al. experimented to prove that the bandwidth is enhanced, and the capability of practical application in robotics is clear. This paper experimented to identify the three parameters such as spring coefficient, damping coefficient, and contractible element force. Besides, the dynamic characterization of an in-house fabricated PAM. In this study, a model was developed which is used for a closed-loop system for controlling position and force [3]. In Ref. [4], the PAM's model static characteristics and experimented with to validate with the other models. Next, Ref. [5] used different methods such as the lumped parameter phenomenological model to simulate the dynamic characteristic of the PAM. Ref. [6] experimented to validate the proposed model for predicting the dynamic hysteresis behavior depending on both rate and load effects. This research offers an accurate position control for a PAM. Generally, a nonlinear force can cause the motion of PAM depending on the pressure and deformation. Therefore, Ref. [7] investigated the influence of various loading on the system. Moreover, as presented, PAM systems usually have nonlinearities and uncertainties which brings disadvantages for both modeling precise dynamics and designing controllers. Therefore, Ref. [8] proposed a neuroadaptive nonlinear robust controller to test the stability of the closed-loop system and validate the effectiveness of the proposed system. Based on the reasons above, this paper presents the friction model of the PAM. Then, based on the Berg model the frictional force curve concerning displacement is established. Next, to verify the complex stiffness model of the PAM, a test rig is conducted. The experimental results reveal that the hysteresis loop is enhanced as there is a development of the frequency, showing clearly the effects of the viscoelastic phenomenon on the restoring force of the PAM. The paper is structured as follows, section 2 illustrates the nonlinear dynamic model of the PAM. The test rig is shown in section 3, and some conclusion is drawn in section 4.

II. FRICTIONAL MODEL OF PAM

A McKibben-based muscle is designed by an inner rubber bellow and the outside being a fiber layer that is wrapped around the rubber bellow for improving the strength. During the process of contraction and extension of the PAM, it exists the frictional phenomenon between the fibers (Fig. 1a), fiber, and rubber (Fig. 1b).

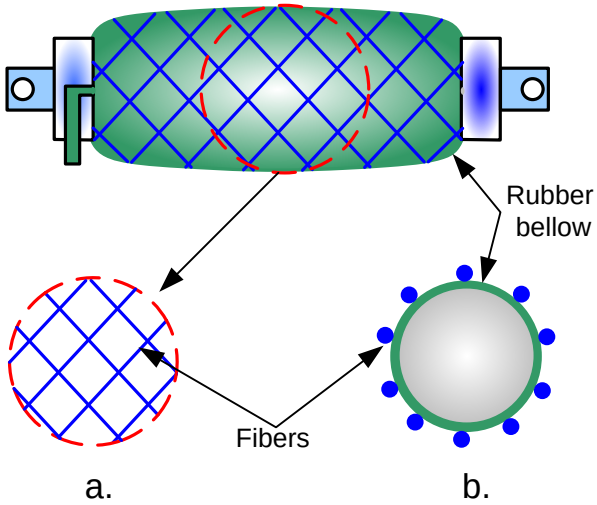

Fig. 1. Physical structure: a. Friction between fibers; b. Friction between fiber and rubber

The friction model offers a nonlinear hysteresis effect on the dynamic response, indicating that an increased stiffness at small displacement amplitudes as well as amplitude-dependent hysteresis will be considered. The frictional force

 EISSN: 2961-872X ● PISSN: 2961-8924 ● DOI: 10.56741/esl.v3i01.551

proposed by Ref. [9] is a good fit for the hysteresis loop when it is excited by the cyclic elongation. This frictional model is expressed as below:

$$F_f = \begin{cases} F_{fs} & x = x_s \\ F_{fs} + \dfrac{x - x_s}{x_2(1-\sigma) + (x - x_s)}(F_{f\max} - F_{fs}) & x > x_s \\ F_{fs} + \dfrac{x - x_s}{x_2(1-\sigma) - (x - x_s)}(F_{f\max} + F_{fs}) & x < x_s \end{cases} \quad (1)$$

herein, the frictional force F_f depends on the displacement x and the reference state (x_s, F_{fs}). Ffmax is the maximum frictional force meanwhile x2 is the displacement at which the frictional force is equal to half F_{fmax}, and α is the auxiliary quantity within (-1:1). As illustrated in Fig. 2, two dashed tangent lines of the hysteresis loop before reaching the extreme displacement present the linear stiffness K_a. The vertical distance between them is equal to 2 F_{fmax}. The displacement (x_2) is calculated by:

$$x_2 = \frac{F_{f\max}}{K_{\max} - K_{la}} \quad (2)$$

The stiffness (K_f) and phase angle (φ_f) are expressed by:

$$K_f = \frac{F_{fo}}{x_o} \quad (3)$$

$$\varphi_f = \frac{\arcsin E_f}{2\pi F_{fo} x_o} \quad (4)$$

where

$F_{fo} = \dfrac{F_{f\max}}{2x_o}\left(\sqrt{x_2^2 + x_o^2 + 6x_2x_o} - x_2 - x_o\right)$ is the steady-state frictional force amplitude

$E_f = 2F_{f\max}\left((2x_o - x_2(1+\psi)^2 \ln\dfrac{x_2(1+\psi) + 2x_o}{x_2(1+\psi)}\right)$ is the energy loss per cycle, $\psi = F_{fo} / F_{f\max}$.

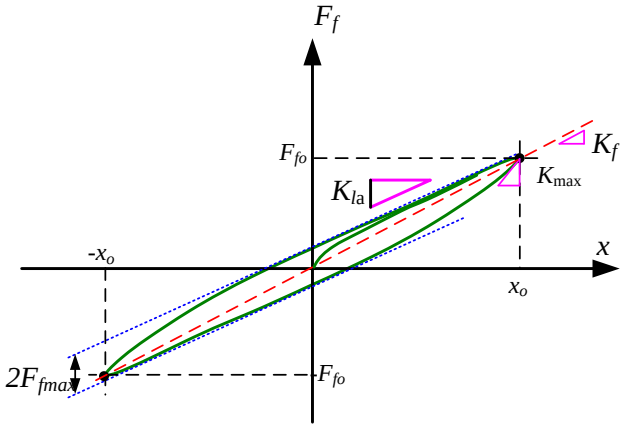

Fig. 2. Frictional force curve concerning displacement

III. TEST RIG

To verify the complex stiffness model of the PAM, a test rig is conducted as shown in Fig. 3. In which the PAM is Festo type DMSP-20-300N-RM-CM (internal diameter 20 mm, natural length 300 mm) and has the maximum contraction ratio of 25% and the initial thread angle of the fiber. Firstly, the bladder of the PAM is pressured to a specified pressure. The one end of the PAM is excited longitudinally by a pneumatic cylinder which is controlled by the proportional valve (MPYE-5-1/8-LF-010-B) meanwhile the other is fixed with the base. The internal pressure of the PAM is adjusted by the pressure regulator. The value of the pressure is monitored versus time via a pressure sensor (BCT-22-10B-V-G1/4-S-30) which ranges from 10 to 10 bar. The displacement of the free end of the PAM is measured by using a linear encoder (RLP50S-1000B-1M) whilst the restoring force generated by the PAM is measured through a load cell (PSD-S1). In addition, an NI 6221 is embedded in the computer to enable Analog-Digital and Digital-Analog conversions. The measurement and control algorithms are realized in the Matlab/Simulink environment.

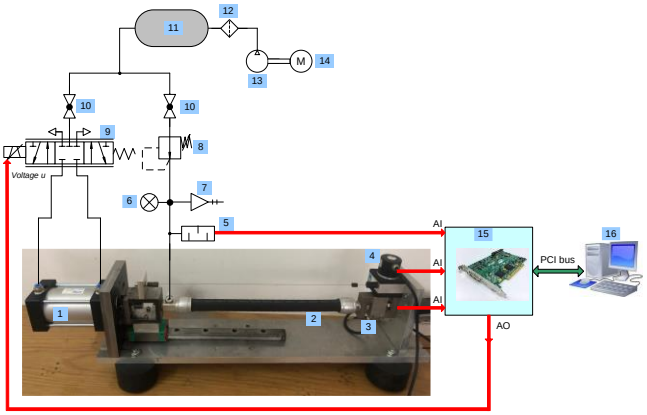

Fig. 3. Experimental setup, (a) schematic diagram of test rig; (b). Diagram of the test system: 1. Pneumatic cylinder; 2. PAM; 3 Load cell; 4. Position sensor; 5. Pressure sensor; 6. Pressure gauge; 7. Safety valve; 8 Pressure regulator; 9. Proportional valve; 10. On-off valve; 11 Air reservoir; 12. Air dryer; 13. Compressor; 14. Electric motor; 15. A/D convector; 16. Computer.

Herein, the free end of the PAM is excited by a sinusoidal signal having a very low frequency (0.005Hz). This means that the effects of the viscoelastic on the restoring force are eliminated because the excited velocity is very small, the experimental data is collected in the quasi-static bench test shown in Fig. 4. The amplitude of the displacement is 20 mm và 10 mm. Through the experimental data, the force-displacement loop (solid line) is plotted as in Fig. 4. According to Fig. 4, the parameters of Berg's model are identified as follows: Ffmax=34 N; x2=0.482 mm. For these values, the predicted curve of the hysteresis loop is denoted by the dashed line, it is interesting that the predicted loop is in agreement with the experiment for the various amplitudes.

As already supposed in Fig 4b for the amplitude of 15 mm and frequency of 0.005 Hz, the frequency is now increased to 1 Hz and 2.5 Hz. The force-displacement loop of the excited frequency of 0.005 Hz is shown once again in Fig. 16 simultaneously, this loop is also compared with hysteresis loops having larger excited frequency (The types of lines are annotated in the panel of the figure). It reveals that the hysteresis loop is enhanced as there is a development of the frequency, showing clearly the effects of the viscoelastic phenomenon on the restoring force of the PAM.

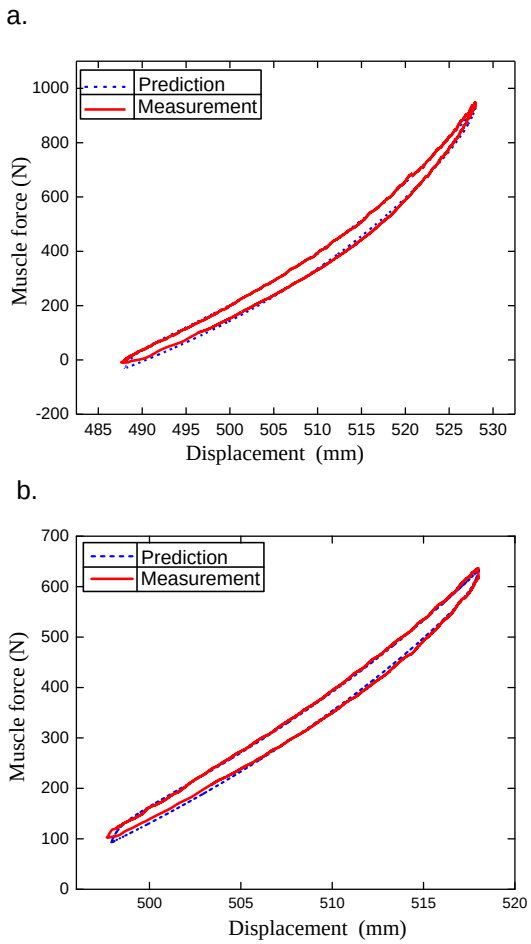

Fig. 4. The hysteresis force-displacement loop: (a) amplitude of 20 mm; (b) Amplitude of 10 mm

IV. Conclusion

PAM is gaining more popularity than its other commercial counterparts because of its high force density, and biological muscle-like characteristics. The researcher must study comprehensively its dynamic nonlinear characteristics. This paper based on Berg's model [9] to investigate the hysteresis feature of the PAM aims to identify the effects of the viscoelastic phenomenon on the restoring force of the PAM. This helps applications related to controlling the PAM, especially Human Robot Interaction and wearable active devices.

References

[1] Cullinan, M. F., Bourke, E., Kelly, K., & McGinn, C. (2017). A McKibben type sleeve pneumatic muscle and integrated mechanism for improved stroke length. *Journal of Mechanisms and Robotics*, *9*(1), 011013.

[2] Cullinan, M. F., Bourke, E., Kelly, K., & McGinn, C. (2020). Dynamic Characterization and Phenomenological Modeling of Sleeve Pneumatic Artificial Muscles. *Journal of Dynamic Systems, Measurement, and Control*, *142*(10), 101005.

[3] Arora, A., Sarkar, D., Sen, S., Kumar, A., & Roy, S. S. (2021, July). Dynamic Characterization and Phenomenological Modelling of Customizable Pneumatic Artificial Muscle. In *2021 IEEE International Conference on Electronics, Computing and Communication Technologies (CONECCT)* (pp. 1-6). IEEE.

[4] Chou, C. P., & Hannaford, B. (1996). Measurement and modeling of McKibben pneumatic artificial muscles. *IEEE Transactions on robotics and automation*, *12*(1), 90-102.

[5] Reynolds, D., Repperger, D., Phillips, C., & Bandry, G. (2003). Modeling the dynamic characteristics of pneumatic muscle. *Annals of biomedical engineering*, *31*, 310-317.

[6] Zhang, Y., Liu, H., Ma, T., Hao, L., & Li, Z. (2021). A comprehensive dynamic model for pneumatic artificial muscles considering different input frequencies and mechanical loads. *Mechanical Systems and Signal Processing*, *148*, 107133.

[7] Sárosi, J., Biro, I., Nemeth, J., & Cveticanin, L. (2015). Dynamic modeling of a pneumatic muscle actuator with two-direction motion. *Mechanism and Machine Theory*, *85*, 25-34.

[8] Chen, Y., Sun, N., Liang, D., Qin, Y., & Fang, Y. (2021). A neuroadaptive control method for pneumatic artificial muscle systems with hardware experiments. *Mechanical systems and signal processing*, *146*, 106976.

[9] Berg, M. (1997). A model for rubber springs in the dynamic analysis of rail vehicles. *Proceedings of the Institution of Mechanical Engineers, Part F: Journal of Rail and Rapid Transit*, *211*(2), 95-108.

 EISSN: 2961-872X ● PISSN: 2961-8924 ● DOI: 10.56741/esl.v3i01.551